SCIENTIFIC REPORTS

OPEN

Redox-Active Ferrocene grafted on H-Terminated Si(111): Electrochemical Characterization of the Charge Transport Mechanism and Dynamics

Received: 10 January 2019
Accepted: 7 June 2019
Published online: 19 June 2019

Claudio Fontanesi[1,2], Enrico Da Como[2], Davide Vanossi[3], Monica Montecchi[1], Maria Cannio[1], Prakash Chandra Mondal[4], Walter Giurlani[5], Massimo Innocenti[5] & Luca Pasquali[1,6,7]

Electroactive self-assembled monolayers (SAMs) bearing a ferrocene (Fc) redox couple were chemically assembled on H-terminated semiconducting degenerate-doped *n*-type Si(111) substrate. This allows to create a Si(111)|organic-spacer|Fc hybrid interface, where the ferrocene moiety is covalently immobilized on the silicon, *via* two alkyl molecular spacers of different length. Organic monolayer formation was probed by Laser Ablation-Inductively Coupled Plasma-Mass Spectrometry (LA-ICP-MS) and X-ray photoelectron spectroscopy (XPS) measurements, which were also used to estimate thickness and surface assembled monolayer (SAM) surface coverage. Atomic force microscopy (AFM) measurements allowed to ascertain surface morphology and roughness. The single electron transfer process, between the ferrocene redox probe and the Si electrode surface, was probed by cyclic voltammetry (CV) measurements. CVs recorded at different scan rates, in the 10 to 500 mV s^{-1} range, allowed to determine peak-to-peak separation, half-wave potential, and charge-transfer rate constant (K_{ET}). The experimental findings suggest that the electron transfer is a one electron quasi-reversible process. The present demonstration of surface engineering of functional redox-active organometallic molecule can be efficient in the field of molecular electronics, surface-base redox chemistry, opto-electronic applications.

Over the past decades, surface-confined nanometric electroactive molecular assemblies have been the subject of key research, which play a major role in understanding redox processes[1–7]. Electroactive materials offer several advantages which include molecular structure-electronic properties correlation and tunability[8–15]. In particular, silicon based hybrid systems are of paramount interest allowing to combine the typical semiconducting properties of Si and the flexible functionalities proper of the organic materials[16–19]. Successful designed molecular architectures produce surface-based sensors, catalytic active surfaces, molecular devices, energy storage, to name a few. Among the redox-active moieties, ferrocene-based derivatives form a class of attractive organic compounds, which can be considered as model systems. This is due to ferrocene structural stability, aromaticity, ease of modification, associated to a reversible single electron transfer process (Fc^+/Fc), low oxidation/reduction potential, and easy to prepare self-assembled monolayers (SAMs)[20,21]. In view of the above fascinating behaviour, ferrocene based SAMs could be exploited as memory elements, where the ferrocene redox centre is used as the charge storage unit and considering the molecule in the neutral or oxidized form as the two states of a bit[22]. This

[1]DIEF, University of Modena and Reggio Emilia, via Vivarelli 10, 41125, Modena, Italy. [2]Department of Physics, University of Bath, Claverton Down, Bath, BA2 7AY, United Kingdom. [3]DSCG, University of Modena and Reggio Emilia, via Campi 183, 41125, Modena, Italy. [4]Department of Chemistry, Indian Institute of Technology, Kanpur, 208016, India. [5]Department of Chemistry, University of Firenze, via della Lastruccia 3, 50019, Sesto Fiorentino, FI, Italy. [6]IOM-CNR Institute, Area Science Park, SS 14 Km, 163.5, Basovizza, 34149, Trieste, Italy. [7]Department of Physics, University of Johannesburg, P.O. Box 524, Auckland, Park, 2006, South Africa. Correspondence and requests for materials should be addressed to C.F. (email: claudio.fontanesi@unimore.it)

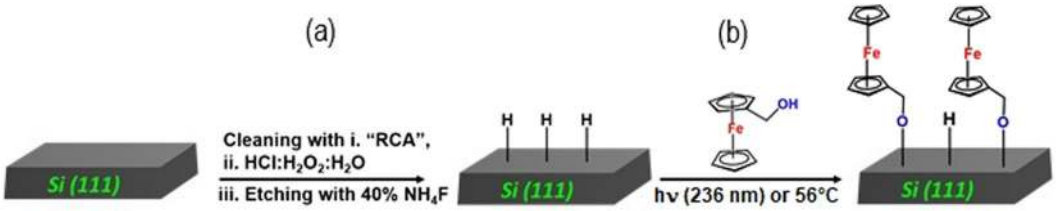

Figure 1. Illustration of the surface modification of the H-terminated silicon substrates. The process involves two steps. Step (**a**): (i) cleaning the silicon (111) substrates with RCA, and $HCl:H_2O:H_2O$ (iii) etching with 40% NH_4F (pH = 2, obtained by addition of few drops of concentrated sulfuric acid) to achieve H-terminated silicon. Step (**b**) covalent grafting of hydroxymethyl ferrocene on H-terminated silicon.

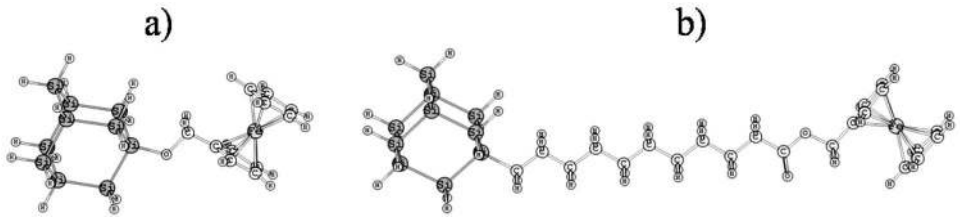

Figure 2. Schematic representation of the molecular architectures grafted on the Si(111) surface (the silicon surface is approximated as a cluster of ten silicon atoms whose dangling valences are saturated by hydrogens): (**a**) Si—Me—Fc (**b**) Si—UA—Fc. The relevant cartesian coordinates, are available in the Supporting Information[36].

kind of supramolecular architectures were experimentally characterized in an extensive way as far as concerns the electron transfer ET process[19,21,23–27], while from a theoretical point of view the fundamental knowledge of the ET dynamics, at an hybrid interface, is a subject yet open for discussion[20,28,29]. Indeed, most of the studies so far refer to ferrocene-terminated alkane thiols attached to a gold substrate. For example, a recent study by Wong *et al*. show that Fc-alkanethiol SAMs form strong ion pairs in the oxidized state which increase the chain length by more than 1 nm as probed by combining electrochemical and XPS measurements[30]. However, techniques to assemble the ferrocene derivative on the different substrates may vary depending on the functional group available. Thus, the functionalization of a molecule-electrode for studying interfacial properties needs a special attention. Different fruitful methodologies exist for the creation of hybrid interfaces, relying on the covalent grafting of functional organic molecules, organometallics, inorganic complexes and these are generally based on ultra-high vacuum (UHV) depositions[31–34], wet chemistry[1,19], electrochemical based methodologies[35]. Fc-SAMs other than the thiolated groups, especially Fc containing alcohol groups are basically unexplored. In this paper, we focus on silicon-based interfaces, as silicon is a linchpin material for micro-electronic industries and can be chemically functionalized by covalent grafting of the ferrocene derivatives. The wet chemistry method is the most widely used technique, due to the simple lab procedures and the vast number of reactive groups that can be grafted on the varied substrates. Herein, we study laboratory synthesized ferrocene derivatives covalently grafted on freshly prepared H-terminated silicon (111) substrate (Fig. 1).

This study is carried out by varying the length of the chain (spacer) linking the ferrocene moiety to the surface: (1) methanol-ferrocene directly grafted on the surface (2) ferrocene grafted through a 1-iodoundecanoic acid (UA) monolayer, Fig. 2.

Formation, surface coverage, elemental analysis, electron-transfer kinetics of the Fc-SAMs on H-terminated silicon was ensured by X-ray Photoelectron Spectroscopy (XPS), Laser Ablation-Inductively Coupled Plasma-Mass Spectrometry (LA-ICP-MS), cyclic voltammetry (CV) measurements. The experimental outcome is compared to theoretical results concerning the dynamics of the electron transfer as obtained by application of the Marcus theory[36]. From the theoretical point of view, our main goal is to verify if Marcus theory[37] is correctly capable in reproducing ET rate constants obtained experimentally. Note that, some recent works[20,28] were devoted to point out that the Marcus model, which describes the ET dynamics in the incoherent limit[38], fails to give a correct prediction of the ET rate constants. Particular attention is also devoted to draw a parallelism between the striking differences observed for the ET dynamics, probed by CV measurements, in the case of ferrocene covalently immobilized, or in bulk solution, in the case of SAMs of comparable thickness.

Results and Discussion

XPS analysis. XPS measurements were performed on the freshly prepared Si—Me—Fc and Si—UA—Fc surfaces. Figure 3a sets out the details of the XPS signal in the 690–740 eV range, the region of Fe 2p binding energy. The spectra show prominent features at 707.8 eV and 721 eV, which are associated with Fe $2p_{3/2}$, $2p_{1/2}$, respectively of Fc-CH_2-OH deposited on H-Si(111)[39–41]. Experimental data show a spin orbit splitting at 13.2 eV and a similar spin-orbit splitting was reported with other Fe^{II}-polypyridyl complexes[39]. The broad shoulder at about 711 eV is

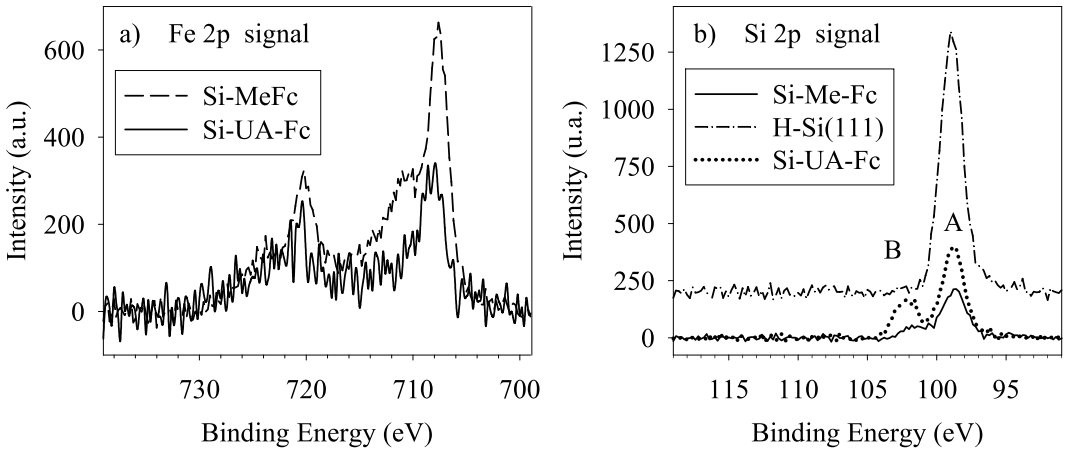

Figure 3. (**a**) Fe 2p XPS signal for Si−Me−Fc (continuous line) and Si−UA−Fc (dotted line) surfaces. (**b**) Si 2p levels for the pristine surface (broken-dotted line) and for Si−Me−Fc (continuous line) and Si−UA−Fc (dotted line) surfaces.

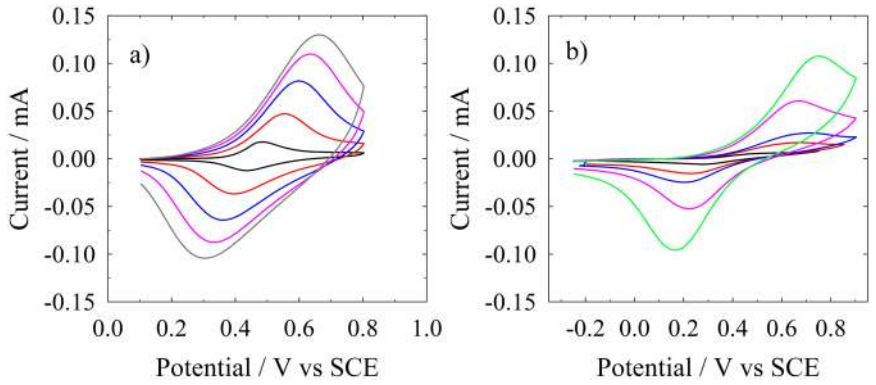

Figure 4. Cyclic voltammetry curves, 0.1 M TBATBF in ACN: (**a**) Si−Me−Fc, scan rate: 10 (black), 50 (red), 100 (blue), 200 (pink), 500 (gray) mV s^{-1} (**b**) Si−UA−Fc, scan rate: 10 (black), 50 (red), 100 (blue), 200 (pink), 500 (gray) mV s^{-1}.

instead related to the presence of some amount of ferrocenium, which has been typically observed for these systems, either due to the manipulation of the samples or to the irradiation of the films under the X-ray beam[39–41]. A shake-up satellite contributes to the high binding energy tail of Fe $2p_{3/2}$, at about 714 eV[39–41]. In Fig. 3b the Si 2p is shown. The pristine surface presents a single peaked structure centred at 99 eV, indicating no traces of surface oxidation[42,43]. Indeed, a non-negligible amount of oxidised Si is found on the Si−UA−Fc surface. To assess quantitatively the Si(111) surface coverage, the attenuation of the Si 2p signal from the substrate was considered, assuming an inelastic mean free path (IMFP), λ, of 31 Å (at the kinetic energy of the Si photoelectrons of 1150 eV) in the organic layer[44]. The film effective thickness was derived applying the standard formula $d = \lambda \cos\theta \ln\left(I_{Si2p,0}/I_{Si2p,d}\right)$, where θ = 44.1° is the average emission angle and $I_{Si2p,0(d)}$ are the peak intensities of the Si2p levels from the bare substrate and from the covered sample with a film of effective thickness d, respectively[45]. We obtained an effective thickness, d = 32 Å (with a tilt angle of about 80 degrees with respect to the silicon surface) and 16 Å (with a tilt angle of about 68 degrees with respect to the silicon surface) for the Si−Me−Fc and Si−UA−Fc surfaces, respectively. This result may suggest, by comparison with optimized structures and relevant geometrical parameters obtained by DFT results (shown in Fig. 1), that the coverage with Si−Me−Fc is about 2 to 3 monolayers, while the coverage corresponds to a single monolayer in the case of Si−UA−Fc. This also accounts for the reduced intensity of Fe 2p structures in Si−UA−Fc compared to Si−Me−Fc.

Electrochemical studies. Attachment of the redox-active ferrocene moiety and its electrochemical kinetic studies were performed by conventional CV measurements. Figure 4a,b shows CV curves as a function of the scan rate, the latter are recorded by using the Si−Me−Fc and Si−UA−Fc interfaces as the working electrode. In the case of the Si−Me−Fc a one electron oxidation process was observed at +0.45 V, while reduction process occurs at +0.35 V (vs. SCE), compare Fig. 4a. As expected the oxidation process shifted towards more positive potential, while reduction process shifted towards more negative potential upon increasing the scan rates. Indeed, the peak-to-peak CV separation (ΔE_p) increases with the scan rate (compare Fig. 3SI in the Supporting

		SiMeFc	SiUAFc
Laviron[47]	k_{ET}/s^{-1}	0.84	0.026
	α	0.61	0.69
CV Simulation[b]	E°/V vs SCE	0.46	0.59
	k_{ET}/s^{-1}	0.98	0.009
	α	0.45	0.40
	Γ/mol cm^{-2}	3.6×10^{-10}	4.0×10^{-10}
i_p *vs.* $ln(\nu)$[48]	Γ/mol cm^{-2}	4.3×10^{-10}	4.7×10^{-10}

Table 1. Standard potential (E°), molecular surface coverage (Γ), ET rate constant (k_{ET}) and charge transfer coefficient (α) As obtained by CV data. [a]CH Instrument simulation program version 9.24.

Information). From a qualitative point of view, the cyclic voltammetry results suggest a quasi-reversible in nature oxidation process of the grafted ferrocene, this because the peak potentials of the forward and backward scan are always shifted by a not-negligible voltage value, while a true reversible process should feature the same (reduction and oxidation) potential values[3]. Using the cyclic voltammetry data, surface coverage of the Si−Me−Fc monolayer was determined at 4.3×10^{-10} mol/cm^2 considering i_p vs. $\ln(\nu)$[46]. For a short molecule, this surface coverage value indicate that monolayers are reasonably well packed[47–49]. Linear behaviour of the Faradic peak current as a function of the scan rates strongly indicate that Fc−CH_2−OH successfully covalently grafted on the silicon substrate. The ratio between anodic and cathodic peak current was experimentally found just larger than one (again in agreement with a quasi-reversible behaviour). Figure 4b sets out CVs recorded in the case of the Si−UA−Fc electrode, the overall behaviour is similar to that one of the shorter molecular-spacer with a more prominent less-reversible behaviour: larger ΔE_p values and smaller current values with respect to the Si−Me−Fc system. We further investigated full width at half maximum (FWHM) at different scan rates, which were found higher than the ideal Nernstian behaviour of 90.6/n mV. This deviation can be ascribed to stray electrostatic effects induced by adjacent charged species not involved in the redox process[50].

Table 1 sets out the experimental parameters obtained by treatment of data in the Fig. 4a,b. A substantial large variation is observed in the electron-transfer rate constant, $\boldsymbol{K_{ET}}$, experimental values present in the literature relevant to ferrocene moieties grafted on Si single crystal surfaces (ranging between 4500 to 3 s^{-1}, such a large variation indicates a high sensitivity of electrochemical measurements to the structure, which is a function of the chemical preparation, of these hybrid interfaces)[25,43,44,47–49,51]. Note that all the elaboration of the experimental electrochemical evidence (details are reported in the Supporting Information) was carried out assuming a one electron single step charge transfer mechanism, allowing for an effective rationalization of the experimental overall picture. Which is the same mechanism underlying the theoretical analysis reported in ref.[34], comparing the experimental values of charge transfer rate constants with the theoretical ones, we can conclude that the charge transfer dynamics follows a Marcus mechanism in the case of the Si−Me−Fc, while in the case of Si−UA−Fc the agreement is not so good (the experimental charge transfer rate constant is much larger than the theoretical one. Theoretical values obtained by first principle calculations carried out within the Marcus paradigm yield $k_{ET} = 77.8\ s^{-1}$ and $k_{ET} = 1.3 \times 10^{-9}\ s^{-1}$ for Si−Me−Fc and Si−UA−Fc, respectively[36]). Experimentally, the Si−Me−Fc electrode shows a more reversible behavior with respect to the Si−UA−Fc one, as can be inferred by i) standard potential values (the E° of Si−Me−Fc is smaller than the Si−UA−Fc one, compare the data in Table 1) ii) the peak-to-peak potential separation (ΔEp) is smaller for Si−Me−Fc than for the Si−UA−Fc: for the same value of scan rate, compare for instance the potential peak-to-peak separation in Fig. 4a (Si−Me−Fc, at 500 mV s^{-1} scan rate gray curve) ΔEp = 300 mV, while Fig. 4b (Si−UA−Fc, at 500 mV s^{-1} scan rate gray curve) ΔEp = 600 mV indicating a more reversible behavior of the Si−Me−Fc than for the Si−UA−Fc.

Atomic force microscopy. To assess the influence of the functionalization process on the morphology of the surface, AFM images were recorded. Figure 5a shows the surface morphology of the Si−UA−Fc hybrid interface, which is the sample subjected to the largest number of electrochemical and chemical treatment steps. Figure 5b sets out the profile (section measured at 2.5 mm height with respect to the vertical axis) in the middle of the scan relevant to Fig. 5a morphology: the sample appears rather flat at the nanoscale, confirming that the functionalization and the sustained treatments did not end up in any dramatic damage of the surface.

For the sake of comparison AFM measurements were performed also on the Si-Me-Fc sample, on the silicon functionalized with the undecanoic acid (Si-UA) and bare Si (roughness values, images and surface profiles are reported in the Supporting Information). The root mean square (RMS) roughness, R_{rms}, value was used as indication of the surface coarseness induced by the different treatments. The following R_{rms} values are obtained: Si 1.60 (±0.2) nm, Si-UA 1.49 (±0.15) nm, Si-Me-Fc 0.90 (±0.1) nm, Si-UA-Fc 1.41 (±0.15) nm. The variations of R_{rms} in the different samples are minimal and comparable with the roughness of the bare pristine silicon substrate; indeed, we can conclude that the functionalization treatments do not result in surfaces with higher roughness with respect to the original pristine silicon.

Conclusions

Redox active ferrocene was covalently immobilized onto the silicon surface via SiOC and SiC covalent bonds. From the experimental point of view, our electrochemical experimental results are in line with the evidence reported by Simonet[52], Zannoni *et al.*[41,49] and Calborean[21], when dealing with similar hybrid interfaces. The striking result is that the connection of the iron redox couple via a chain of single (N.B: not conjugated) covalent

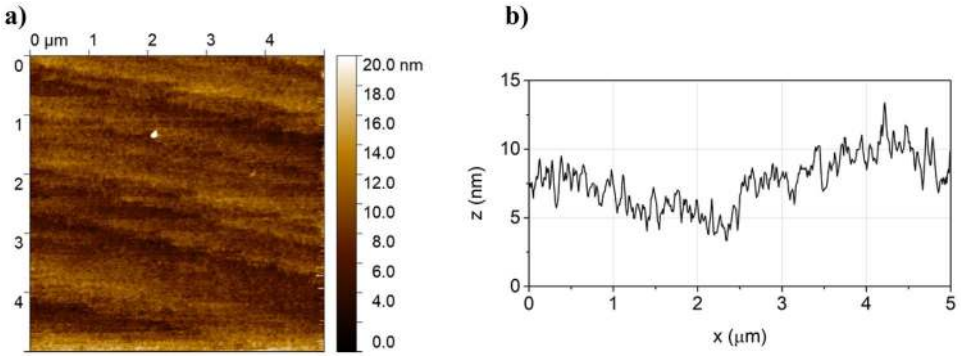

Figure 5. AFM scans of the Si-UA-Fc sample (scan area 5.0 µm × 5.0 µm): (**a**) surface morphology (**b**) heights profile related to the horizontal mid cross section.

bonds (even in the case of a long, in principle not conducting, alkyl chain) acts as an on/off switch on the ET process involving the ferrocene: the charge of the interface is driven by the external applied potential (bias), which can be switched on (charged, i.e. oxidized ferrocene) and off (discharged, i.e. neutral ferrocene) following the application of a suitable value of the bias. Moreover, the results here reported show that the efficiency of the on/off (charge/discharge) process is a function of the structure of the linker placed between the redox centre (ferrocene) and the electrode surface (in this case silicon). This result is at variance with respect to the case of an alkyl SAM functionalized electrode surface (1decanethiol on Au), but featuring the ferrocene in bulk solution: in this case the Faradaic current is almost zero although the distance between the ferrocene and the electrode surface, as well as the chemical nature of the spacer, are quite similar[4]. Moreover, a semi-quantitative agreement between the experimental and theoretical values is found for the "short spacer" ferrocene derivative, also XPS data reveals well-defined signals including elemental compositions. For the Si−UA−Fc system a much larger, than theoretically expected, experimental K_{ET} value is found. A result in line with findings recently discussed in the literature, where high current values are found (i.e. CVs featuring evident redox current peaks) even dealing with long saturated alkyl-carbon chains, where a non-conducting behaviour is expected[3,20,22,28]. Compare the results discussed in A. Nitzan, *Chemical dynamics in condensed phases relaxation, transfer and reactions in condensed molecular systems*: page 600 Figure 16.9. Eventually, the experimental charge transfer rate constant for the Si-Me-Fc electrode, $K_{ET} = 0.98\ s^{-1}$, is found to be smaller than the theoretical value of $77.8\ s^{-1}$, the latter was obtained by application of the Marcus theory, which represents a theoretical upper ideal limit.

As a whole, it must be noted that surface engineering with ferrocene immobilized moieties was successfully achieved on H-terminated silicon substrate, a route which is promising in building and tailoring nanoscale devices for applications in the field of molecular electronics, spintronics, photonics, catalytic properties.

Materials and Methods

Materials and Reagents. All the reagents used in this work are from Sigma, unless otherwise stated (compare the synthetic details in the Supporting Information), and used as received without any further purification. Highly n-doped silicon substrates (degenerate) with a resistivity <0.010 ohm.cm and thickness in the 475 to 525 µm range, were purchased from Siltronix.

Preparation and functionalization of H-terminated Si(111) surface. Silicon substrates were cleaned by sonication in n-hexane, acetone, then ethanol (15 min each) and then, dried under a N_2 stream. Hydrogen terminated Si(111) surfaces [H-Si(111)] were prepared following the procedure described by Dumas and Kato[53,54]. A series of acid and basic hot bath cleaning steps were performed followed by a final NH_4F treatment[54]. Functionalization of the H-terminated Si(111) surface was carried out using a standard Schlenk-line procedure for reaction in inert atmosphere. Photo-induced grafting of was carried out by covering the H-terminated Si(111) surface with Fc-CH_2OH and irradiating the sample for 1 h with a power of ~35 mW cm^{-2} using a quartz–iodine lamp with the main emission peak at 236 nm. The flask was heated above the melting point of Fc-CH_2OH, at 56 °C.

Electrochemical measurements. Cyclic voltammetry (CV) measurements were performed using CHI 660 A and Metrohm Autolab Pgstat 128 N potentiostats, in a typical three-electrode electrochemical cell arrangement. Fc-CH_2-OH modified H-terminated Si(111) substrates used as a working electrode (active area = 78 mm^2), a Pt wire and a Saturated Calomel Electrode $Hg/Hg_2Cl_2/KCl_{sat}$ (SCE) electrodes used as the counter and reference electrodes, respectively. Ohmic contacts were made by rubbing indium-gallium (In-Ga) eutectic alloy (495425 Aldrich) on the back of the previously scratched to further improve the contact[51]. 0.1 M tetrabutylammonium tetrafluoroborate (TBATFB) in acetonitrile (ACN) was the base electrolyte.

X-ray photoelectron spectroscopy (XPS) measurements. For XPS measurements, Mg K_α radiation was used from a dual anode non-monochromatic X-ray source (VG-XR3) operated at 15 mA, 15 kV. Spectra were acquired with double-pass cylindrical mirror analyzer (PHI-15-255G) at constant pass energy of 50 eV.

Atomic force microscopy (AFM) measurements. Atomic force microscopy (AFM) (PicoSPM, Molecular Imaging, Tempe, AZ, USA) was used to acquire images of the samples (512 px × 512 px, 5 μm × 5 μm) and evaluate the roughness. The measurements were performed in contact mode with a non-conductive Si_3N_4 triangular cantilever (NP-S10, Veeco, Plainview, NY, USA) with the following features: 0.4–0.7 μm range in depth, 0.12 N/m force constant, 0.5 V force set point and 1.21 l/s speed.

References

1. Allongue, P. *et al*. Organic monolayers on Si(111) by electrochemical method. *Electrochimica Acta* **43**, 2791–2798 (1998).
2. C P. Andrieux, F Gonzalez & Savéant*, J.-M. Derivatization of Carbon Surfaces by Anodic Oxidation of Arylacetates. Electrochemical Manipulation of the Grafted Films, https://doi.org/10.1021/ja9636092 (1997).
3. Eckermann, A. L., Feld, D. J., Shaw, J. A. & Meade, T. J. Electrochemistry of redox-active self-assembled monolayers. *Coordination Chemistry Reviews* **254**, 1769–1802 (2010).
4. Fontanesi, C., Camurri, G. & Tassinari, F. On the co-adsorption process of sodium dodecyl sulfate and sodium dodecylbenzenesulfonate on a 1-decanethiol-functionalized Au electrode, as a corrosion inhibiting mimic process. *J Appl Electrochem* **43**, 101–106 (2012).
5. Mondal, P. C., Mtangi, W. & Fontanesi, C. Chiro-Spintronics: Spin-Dependent Electrochemistry and Water Splitting Using Chiral Molecular Films. *Small. Methods* **2**, 1700313 (2018).
6. Singh, V., Mondal, P. C., Singh, A. K. & Zharnikov, M. Molecular sensors confined on SiOx substrates. *Coordination Chemistry Reviews* **330**, 144–163 (2017).
7. Mondal, P. C., Singh, V. & Zharnikov, M. Nanometric Assembly of Functional Terpyridyl Complexes on Transparent and Conductive Oxide Substrates: Structure, Properties, and Applications. *Acc. Chem. Res.* **50**, 2128–2138 (2017).
8. Fontanesi, C. Entropy change in the two-dimensional phase transition of adenine adsorbed at the Hg electrode/aqueous solution interface. *J. Chem. Soc., Faraday Trans.* **90**, 2925–2930 (1994).
9. Marcaccio, M., Paolucci, F., Fontanesi, C., Fioravanti, G. & Zanarini, S. Electrochemistry and spectroelectrochemistry of polypyridine ligands: A theoretical approach. *Inorganica chimica acta* **360**, 1154–1162 (2007).
10. Fontanesi, C. *et al*. New One-Step Thiol Functionalization Procedure for Ni by Self-Assembled Monolayers. *Langmuir* **31**, 3546–3552 (2015).
11. Loglio, F. *et al*. Cadmium selenide electrodeposited by ECALE: electrochemical characterization and preliminary results by EXAFS. *Journal of Electroanalytical Chemistry* **575**, 161–167 (2005).
12. Guidelli, R., Foresti, M. L. & Innocenti, M. Two-Dimensional Phase Transitions of Chemisorbed Uracil on Ag(111): Modeling of Short- and Long-Time Behavior. *J. Phys. Chem.* **100**, 18491–18501 (1996).
13. Innocenti, M. *et al*. *In situ* atomic force microscopy in the study of electrogeneration of polybithiophene on Pt electrode. *Electrochimica Acta* **50**, 1497–1503 (2005).
14. Foresti, M. L. *et al*. Ternary CdSxSe1-x Deposited on Ag(111) by ECALE: Synthesis and Characterization. *Langmuir* **21**, 6900–6907 (2005).
15. Giovanardi, R., Fontanesi, C. & Dallabarba, W. Adsorption of organic compounds at the aluminium oxide/aqueous solution interface during the aluminium anodizing process. *Electrochimica Acta* **56**, 3128–3138 (2011).
16. Nalwa, H. S. Preface. in *Silicon-Based Material and Devices* (Academic Press, 2001).
17. Shimura, F. *Semiconductor Silicon Crystal Technology*. (Academic Press, 1989).
18. Aswal, D. K., Lenfant, S., Guerin, D., Yakhmi, J. V. & Vuillaume, D. Self assembled monolayers on silicon for molecular electronics. *Analytica Chimica Acta* **568**, 84–108 (2006).
19. Buriak, J. M. Organometallic Chemistry on Silicon and Germanium Surfaces. *Chem. Rev.* **102**, 1271–1308 (2002).
20. Paul, A. *et al*. Distance Dependence of the Charge Transfer Rate for Peptide Nucleic Acid Monolayers. *J. Phys. Chem. B* **114**, 14140–14148 (2010).
21. Calborean, A., Buimaga-Iarinca, L. & Graur, F. DFT charge transfer of hybrid molecular ferrocene/Si structures. *Phys. Scr.* **90**, 055803 (2015).
22. Slinker, J. D., Muren, N. B., Renfrew, S. E. & Barton, J. K. DNA Charge Transport over 34 nm. *Nat Chem* **3**, 230–235 (2011).
23. Chidsey, C. E. D., Bertozzi, C. R., Putvinski, T. M. & Mujsce, A. M. Coadsorption of ferrocene-terminated and unsubstituted alkanethiols on gold: electroactive self-assembled monolayers. *J. Am. Chem. Soc.* **112**, 4301–4306 (1990).
24. Wayner, M. D. D. & A. Wolkow, R. Organic modification of hydrogen terminated silicon surfaces 1. *Journal of the Chemical Society, Perkin Transactions 2* **0**, 23–34 (2002).
25. Roth, K. M. *et al*. Measurements of Electron-Transfer Rates of Charge-Storage Molecular Monolayers on Si(100). Toward Hybrid Molecular/Semiconductor Information Storage Devices. *J. Am. Chem. Soc.* **125**, 505–517 (2003).
26. Fabre, B. & Hauquier, F. Single-Component and Mixed Ferrocene-Terminated Alkyl Monolayers Covalently Bound to Si(111) Surfaces. *J. Phys. Chem. B* **110**, 6848–6855 (2006).
27. Hauquier, F., Ghilane, J., Fabre, B. & Hapiot, P. Conducting Ferrocene Monolayers on Nonconducting Surfaces. *J. Am. Chem. Soc.* **130**, 2748–2749 (2008).
28. Nitzan, A. *Chemical dynamics in condensed phases relaxation, transfer and reactions in condensed molecular systems*. (Oxford University Press, 2006).
29. Benedetti, L., Gavioli, G. B. & Fontanesi, C. A theoretical and topological study on the electroreduction of chlorobenzene derivatives. *J. Chem. Soc., Faraday Trans.* **86**, 329–334 (1990).
30. Wong, R. A., Yokota, Y., Wakisaka, M., Inukai, J. & Kim, Y. Discerning the Redox-Dependent Electronic and Interfacial Structures in Electroactive Self-Assembled Monolayers. *J. Am. Chem. Soc.* **140**, 13672–13679 (2018).
31. Lopinski, G. P., Fortier, T. M., Moffatt, D. J. & Wolkow, R. A. Multiple bonding geometries and binding state conversion of benzene/Si(100). *Journal of Vacuum Science & Technology A* **16**, 1037–1042 (1998).
32. Hamers, R. J., Hovis, J. S., Lee, S., Liu, H. & Shan, J. Formation of Ordered, Anisotropic Organic Monolayers on the Si(001) Surface. *J. Phys. Chem. B* **101**, 1489–1492 (1997).
33. Lopinski, G. P., Moffatt, D. J., Wayner, D. D. M. & Wolkow, R. A. Determination of the absolute chirality of individual adsorbed molecules using the scanning tunnelling microscope. *Nature* **392**, 909–911 (1998).
34. Allegretti, F. *et al*. HREELS study of the adsorption mechanism and orientational order of 2-mercaptobenzoxazole on Cu(100). *Surface Science* **539**, 63–71 (2003).
35. Hartig, P., Rappich, J. & Dittrich, T. Engineering of Si surfaces by electrochemical grafting of p-nitrobenzene molecules. *Applied Physics Letters* **80**, 67–69 (2002).
36. Fontanesi, C., Innocenti, M., Vanossi, D. & Da Como, E. Ferrocene Molecular Architectures Grafted on Si(111): A Theoretical Calculation of the Standard Oxidation Potentials and Electron Transfer Rate Constant. *Materials* **10**, 1109 (2017).
37. Marcus, R. A. Electron transfer reactions in chemistry. Theory and experiment. *Reviews of Modern Physics* **65**, 599–610 (1993).
38. May, V. & Kuhn, O. *Wiley: Charge and Energy Transfer Dynamics in Molecular Systems, 3rd, Revised and Enlarged Edition - Volkhard May, Oliver Kuhn*.
39. Leo, L. P. M. D., Llave, E., de la, Scherlis, D. & Williams, F. J. Molecular and electronic structure of electroactive self-assembled monolayers. *The Journal of Chemical Physics* **138**, 114707 (2013).

40. Fischer, A. B., Wrighton, M. S., Umana, M. & Murray, R. W. An x-ray photoelectron spectroscopic study of multilayers of an electroactive ferrocene derivative attached to platinum and gold electrodes. *J. Am. Chem. Soc.* **101**, 3442–3446 (1979).
41. Dalchiele, E. A. *et al*. XPS and electrochemical studies of ferrocene derivatives anchored on n- and p-Si(100) by Si–O or Si–C bonds. *Journal of Electroanalytical Chemistry* **579**, 133–142 (2005).
42. Himpsel, F. J., McFeely, F. R., Taleb-Ibrahimi, A., Yarmoff, J. A. & Hollinger, G. Microscopic structure of the SiO2/Si interface. *Phys. Rev. B* **38**, 6084–6096 (1988).
43. Hirose, K., Nohira, H., Azuma, K. & Hattori, T. Photoelectron spectroscopy studies of SiO2/Si interfaces. *Progress in Surface Science* **82**, 3–54 (2007).
44. Tanuma, S., Powell, C. J. & Penn, D. R. Calculations of electron inelastic mean free paths. V. Data for 14 organic compounds over the 50–2000 eV range. *Surf. Interface Anal.* **21**, 165–176 (1994).
45. Briggs, D. & Seah, M. P. *Practical Surface Analysis,Auger and X-ray Photoelectron Spectroscopy*. **1**, (John Wiley & Sons, 1990).
46. Zigah, D. *et al*. Tuning the Electronic Communication between Redox Centers Bound to Insulating Surfaces. *Angewandte Chemie International Edition* **49**, 3157–3160 (2010).
47. Decker, F. *et al*. Electrochemical Reversibility of Vinylferrocene Monolayers Covalently Attached on H-Terminated p-Si(100). *J. Phys. Chem. B* **110**, 7374–7379 (2006).
48. Lu, M., He, T. & Tour, J. M. Surface Grafting of Ferrocene-Containing Triazene Derivatives on Si(100). *Chem. Mater.* **20**, 7352–7355 (2008).
49. Marrani, A. G. *et al*. Functionalization of Si(100) with ferrocene derivatives via "click" chemistry. *Electrochimica Acta* **53**, 3903–3909 (2008).
50. Brown, A. P. & Anson, F. C. Cyclic and differential pulse voltammetric behavior of reactants confined to the electrode surface. *Anal. Chem.* **49**, 1589–1595 (1977).
51. Lehmann, V. & Föll, H. Formation Mechanism and Properties of Electrochemically Etched Trenches in n-Type Silicon. *Journal of The Electrochemical Society* **137**, 653–659 (1990).
52. Jouikov, V. & Simonet, J. Novel Method for Grafting Alkyl Chains onto Glassy Carbon. Application to the Easy Immobilization of Ferrocene Used as Redox Probe. *Langmuir* **28**, 931–938 (2012).
53. Mazzara, C. *et al*. Hydrogen-terminated Si(111) and Si(100) by wet chemical treatment: linear and non-linear infrared spectroscopy. *Surface Science* **427–428**, 208–213 (1999).
54. Kato, H. *et al*. Preparation of an Ultraclean and Atomically Controlled Hydrogen-Terminated Si(111)-(1 × 1) Surface Revealed by High Resolution Electron Energy Loss Spectroscopy, Atomic Force Microscopy, and Scanning Tunneling Microscopy: Aqueous NH 4 F Etching Process of Si(111). *Japanese Journal of Applied Physics* **46**, 5701–5705 (2007).

Acknowledgements

PCM thanks European Union for Marie-Curie Post-doctoral Fellowship (H2020-MSCA-2015-706238) and acknowledges research support from the Director, and the HOD, Department of Chemistry, IIT Kanpur. Prof. Andrea Cornia, DSCG, Univ. of Modena and Reggio Emilia is kindly acknowledged for helpful discussion.

Author Contributions

C.F., D.V. and M.I. designed and planned the scientific work; C.F. and E.D.C. discussed the experimental set-up and results; M.M., M.C., P.C.M., W.G. and L.P. made the experimental measurements, C.F. wrote the manuscript; D.V., L.P., M.I. and L.P. discussed and revised the manuscript.

Additional Information

Supplementary information accompanies this paper at https://doi.org/10.1038/s41598-019-45448-w.

Competing Interests: The authors declare no competing interests.

Publisher's note: Springer Nature remains neutral with regard to jurisdictional claims in published maps and institutional affiliations.